

- Cartwright, R. A., Robinson, M. R. G., Glashan, R. W., Gray, B. K., Hamilton-Stewart, P., Cartwright, S. C., and Barnham-Hall, D. (1983). Does the use of stained maggots present a risk of bladder cancer to coarse fishermen? *Carcinogenesis* **4**:111–113.
- Dehouck, M. P., Jolliet-Riant, P., Brée, F., Fruchart, J. C., Cecchelli, R., and Tillement, J. P. (1992). Drug transfer across the blood–brain barrier: Correlation between *in vitro* and *in vivo* models. *J. Neurochem.* **58**:1790–1797.
- Dohgu, S., Yamauchi, A., Takata, F., Sawada, Y., Higuchi, S., Naito, M., Tsuruo, T., Shirabe, S., Niwa, M., Katamine, S., and Kataoka, Y. (2004). Uptake and efflux of quinacrine, a candidate for the treatment of prion diseases, at the blood–brain barrier. *Cell. Mol. Neurobiol.* **24**:205–217.
- Doh-Ura, K., Iwaki, T., and Caughey, B. (2000). Lysosomotropic agents and cysteine protease inhibitors inhibit scrapie-associated prion protein accumulation. *J. Virol.* **74**:4894–4897.
- Frostell-Karlsson, A., Remaeus, A., Roos, H., Andersson, K., Borg, P., Hamalainen, M., and Karlsson, R. (2000). Biosensor analysis of the interaction between immobilized human serum albumin and drug compounds for prediction of human serum albumin binding levels. *J. Med. Chem.* **43**:1986–1992.
- Ishikawa, K., Doh-ura, K., Kudo, Y., Nishida, N., Murakami-Kubo, I., Ando, Y., Sawada, T., and Iwaki, T. (2004). Amyloid imaging probes are useful for detection of prion plaques and treatment of transmissible spongiform encephalopathies. *J. Gen. Virol.* **85**:1785–1790.
- Kawatake, S., Nishimura, Y., Sakaguchi, S., Iwaki, T., and Doh-ura, K. (2006). Surface plasmon resonance analysis for the screening of anti-prion compounds. *Biol. Pharm. Bull.* **29**:927–932.
- Kim, C.-L., Karino, A., Ishiguro, N., Shinagawa, M., Sato, M., and Horiuchi, M. (2004). Cell-surface retention of PrPC by anti-PrP antibody prevents protease-resistant PrP formation. *J. Gen. Virol.* **85**:3473–3482.
- Klunk, W. E., Bacskai, B. J., Mathis, C. A., Kajdasz, S. T., McLellan, M. E., Frosch, M. P., Debnath, M. L., Holt, D. P., Wang, Y., and Hyman, B. T. (2002). Imaging Abeta plaques in living transgenic mice with multiphoton microscopy and methoxy-X04, a systemically administered Congo red derivative. *J. Neuropathol. Exp. Neurol.* **61**:797–805.
- Murakami-Kubo, I., Doh-Ura, K., Ishikawa, K., Kawatake, S., Sasaki, K., Kira, J., Ohta, S., and Iwaki, T. (2004). Quinoline derivatives are therapeutic candidates for transmissible spongiform encephalopathies. *J. Virol.* **78**:1281–1288.
- Nakajima, M., Yamada, T., Kusuhashi, T., Furukawa, H., Takahashi, M., Yamauchi, A., and Kataoka, Y. (2004). Results of quinacrine administration to patients with Creutzfeldt–Jakob disease. *Dement. Geriatr. Cogn. Disord.* **17**:158–163.
- Prusiner, S. B. (1991). Molecular biology of prion diseases. *Science* **252**:1515–1522.
- Race, R. E., Caughey, B., Graham, K., Ernst, D., and Chesebro, B. (1988). Analyses of frequency of infection, specific infectivity, and prion protein biosynthesis in scrapie-infected neuroblastoma cell clones. *J. Virol.* **62**:2845–2849.
- Sandhu, P., and Chipman, J. K. (1990). Bacterial mutagenesis and hepatocyte unscheduled DNA synthesis induced by chrysoidine azo-dye components. *Mutat. Res.* **240**:227–236.
- Sole, G., and Sorahan, T. (1985). Coarse fishing and risk of urothelial cancer. *Lancet* **1**:1477–1479.
- Sorahan, T., and Sole, G. (1990). Coarse fishing and urothelial cancer: A regional case-control study. *Br. J. Cancer* **62**:138–141.
- Tatsuta, T., Naito, M., Oh-hara, T., Sugawara, I., and Tsuruo, T. (1992). Functional involvement of P-glycoprotein in blood–brain barrier. *J. Biol. Chem.* **267**:20383–20391.



Metal complexes with superoxide dismutase-like activity as candidates for anti-prion drug

Tomoko Fukuuchi,^{a,b,*} Katsumi Doh-ura,^c Shin'ichi Yoshihara^b and Shigeru Ohta^a

^aGraduate School of Biomedical Sciences, Hiroshima University, 1-2-3 Kasumi, Minami-ku, Hiroshima 734-8553, Japan

^bFaculty of Pharmaceutical Sciences, Hiroshima International University, 5-1-1 Koshingai, Hiro, Kure, Hiroshima 737-0112, Japan

^cGraduate School of Medicine, Tohoku University, 2-1 Seiryō-cho, Aoba-ku, Sendai 980-8575, Japan

Received 28 July 2006; revised 29 August 2006; accepted 30 August 2006

Available online 20 September 2006

Abstract—Various compounds were evaluated for ability to inhibit the formation of the abnormal protease-resistant form of prion protein (PrP-res) in two cell lines infected with different prion strains. Examination of the structure–activity relationships indicated that compounds with copper-selective chelating ability and whose copper complexes have high SOD-like activity are candidates for anti-prion drug.

© 2006 Elsevier Ltd. All rights reserved.

Transmissible spongiform encephalopathies (TSEs) or prion diseases are a group of fatal neurodegenerative disorders, and their development is associated with accumulation of aggregated proteins, oxidative damage to the brain, and neuronal cell loss. Prion diseases are characterized by the generation of a protein molecule termed PrP^{Sc} (scrapie isoform of the prion protein), which is a conformational variant of the normal host protein, PrP^C (cellular isoform of the prion protein).^{1,2} It is believed that the conversion of PrP^C into PrP^{Sc} is the key event in the pathogenesis of TSEs.

The octapeptide repeat region of the PrP^C binds several copper ions with concentration of the micromolar range^{3,4} and their dissociation constant for the ion is reported to be femtomolar range.⁵ The biological significance of this interaction is not clear, but it is reported that PrP^C has a copper-dependent superoxide dismutase (SOD) activity⁶ and PrP^C may be involved in copper uptake into cells.^{7,8} Recently, there has been increasing interest in the role of metal ions, in particular copper, in prion diseases.^{9,10}

In the early 1970s, it was reported that the copper chelator cuprizone induced prion diseases-like histopa-

thological changes in mice.^{11,12} On the other hand, Sigurdsson et al. recently found that a copper chelator, D-penicillamine, delayed the onset of prion disease in infected mice, and suggested that chelator-based therapy might attenuate the disease.¹³ Copper has been implicated in the pathogenesis of prion disease, but numerous studies have only succeeded in demonstrating the complexity of the effects of copper on the development of prion diseases, and it remains unclear whether this ion promotes or inhibits disease progression.

In the present study, we evaluated the ability of a wide range of compounds¹⁴ to inhibit the formation of the abnormal protease-resistant form of prion protein (PrP-res), using two cell lines, ScN2a cells and F3, infected with different prion strains.^{15,16} We then analyzed the structure–activity relationships to investigate what kinds of structure or biochemical characteristics contribute to anti-prion activity.

Spectrophotometric complexation studies.^{17–19} The complexes were prepared as previously reported.^{20,21} Solutions of 10 mM Cu(ClO₄)₂ and 8-hydroxyquinoline were prepared in H₂O. Cu(II)-chelate formation of 8-hydroxyquinoline was demonstrated by Job's method.^{18,19} The spectrophotometric complexation studies showed that 8-hydroxyquinoline binds in 2:1 ratio with Cu(II) (Fig. 1A). 2,2'-Biquinoline, neocuproine, bathocuproine, 4,4'-dicarboxy-2,2'-biquinoline, porphyrins, cimetidine and D-penicillamine bind in 1:1 ratio with Cu(II) (2,2'-biquinoline, Fig. 1B; others, data not

Keywords: Prion; 2,2'-Biquinoline; Cimetidine; TPEN; Copper; Chelate; Metal complex; SOD activity.

* Corresponding author. Tel./fax: +81 823 73 8573; e-mail: t-fukuu@ps.hirokoku-u.ac.jp

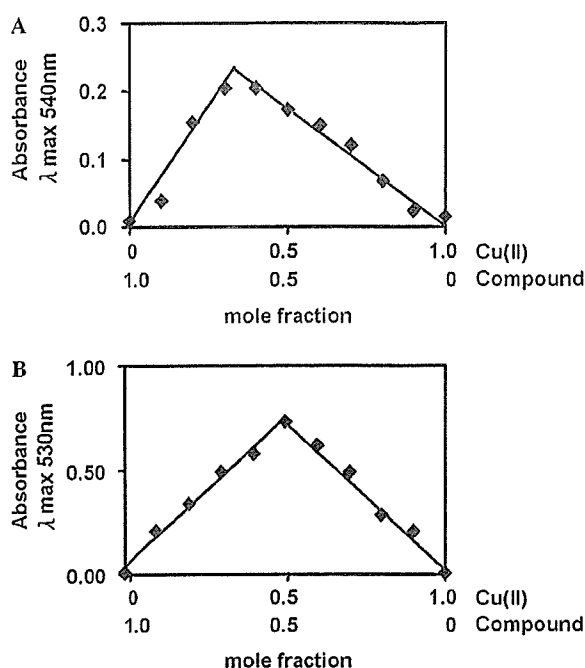


Figure 1. Continuous variation plots for 8-hydroxyquinoline and Cu(II) (A) and 2,2'-biquinoline and Cu(II) (B). (A) 2:1 binding ratio between 8-hydroxyquinoline and Cu(II), (B) 1:1 binding ratio between 2,2'-biquinoline and Cu(II). The plots were obtained by Job's method in aqueous solution.

shown). However, it has been reported that the oxidation state of copper may be altered in the D-penicillamine complex, and the complex prepared in this way contains both Cu(I) and Cu(II).²²

Inhibition of PrP-res formation in ScN2a cells and F3 cells by metal chelators.^{23–26} 1,10-Phenanthroline, 2,2',2''-terpyridine and 8-hydroxyquinoline did not inhibit PrP-res formation within a nontoxic dose range (Table 1), but were cytotoxic at 100 nM. Chelators of this class can chelate a wide variety of metals.

Neocuproine, bathocuproine, 2,2'-biquinoline and 4,4'-dicarboxy-2,2'-biquinoline are highly specific copper chelators. The chelators of this class, except 4,4'-dicarboxy-2,2'-biquinoline, effectively inhibited PrP-res formation in ScN2a cells and F3 cells in a dose-dependent manner (Fig. 2). The concentrations giving 50% inhibition (IC_{50}) of PrP-res formation in ScN2a cells relative to the DMSO-treated or untreated control ranged from 5 to 80 nM (Table 1). These compounds showed no apparent cytotoxicity at concentrations up to 1 μ M. However, neocuproine was ineffective in F3 cells within a nontoxic dose range. Findings from these experiments suggest that compounds having copper-selective chelating ability are more effective inhibitors than non-selective metal-chelating compounds, but not an exclusive factor.

Inhibition of PrP-res formation in ScN2a cells and F3 cells by porphyrins.^{23–26} Porphyrins can form 1:1 stable chelates with various metal ions. The order of stability

for divalent metal ions is $Cu > Fe > Zn > Mn$, regardless of the type of substituents on the porphyrin ring. Porphyrins were effective inhibitors of PrP-res formation, with IC_{50} values ranging from 5 to 320 nM in ScN2a cells and F3 cells (Table 2). And Mn(III)-porphyrins complexes showed higher anti-prion activity than the metal-free compounds (Table 2).

SOD-like activity and correlation with anti-prion activity. It is known that Mn(III)-porphyrin complexes show high SOD-like activity in vitro and in vivo.^{27,28} We thought that SOD-like activity might contribute to the anti-prion activity of such compounds, since the SOD activity of PrP^C is decreased by conversion to PrP^{Sc}. Therefore, we focused on chelators having SOD-like activity. Many low-molecular metal complexes, mainly copper, manganese and iron complexes, have been synthesized and their SOD-like activity examined in vitro and in vivo,^{29–33} and some of them showed activity in vivo.^{34–36} As shown in Table 3, SOD-like activity of these compounds was measured in vitro by our methods.³⁷ The SOD-like activity in cell lysates was significantly increased when these metal-free compounds were added to the cell cultures (data not shown). Therefore, the chelators that showed anti-prion activity formed metal complexes and had SOD-like activity.

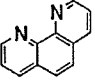
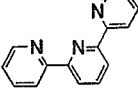
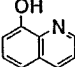
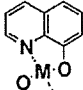
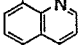
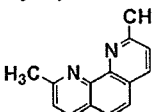
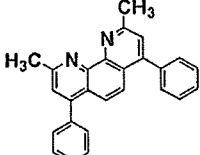
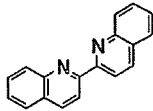
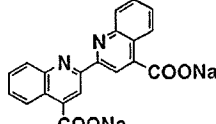
Among these compounds, we chose cimetidine^{34,38} and TPEN³⁹ for further examination, as well as Mn-TCPP (Mn-TBAP), which we had already examined. Cimetidine effectively inhibited PrP-res formation, with IC_{50} values of 5 nM in ScN2a cells and 200 nM in F3 cells. TPEN inhibited PrP-res formation, with IC_{50} values of 5 nM in ScN2a cells and 200 nM in F3 cells.

We found that the compounds, shown in Tables 1 and 2, with higher anti-prion activity in ScN2a cells had higher SOD-like activity (Table 3). Statistical analysis exhibited a significant linear correlation between these two activities ($r = 0.93$) (Fig. 3).

Despite numerous studies, it remains unclear whether copper ions promote¹³ or inhibit⁴⁰ prion disease. In Alzheimer's disease, another neurodegenerative disease, the copper- and zinc-selective chelator clioquinol was effective in decreasing β -amyloid deposits.⁴¹ However, Doh-ura et al. found that clioquinol and related compounds, quinoline hydrochloride, 8-hydroxyquinoline, and 8-acetoxyquinoline, were ineffective in scrapie-infected mouse neuroblastoma (ScNB) cells.²⁵ Thus, chelating drugs that are effective in inhibiting β -amyloid formation may not inhibit the conversion of PrP^C to PrP^{Sc}.

In this study, we evaluated the anti-prion activity of various compounds having metal-chelating ability in order to identify the requirements for anti-prion activity. We found that many, but not all, compounds having selective copper-chelating ability are effective inhibitors of PrP-res formation in ScN2a cells and F3 cells. Thus, copper-selective chelating ability per se may not be essential for anti-prion activity. This idea is supported by the observation that porphyrins chelating manganese

Table 1. Inhibition of PrP-res formation in ScN2a cells and F3 cells by metal chelators

Compound	Structure	Metal(M)	Inhibition PrP-res IC ₅₀ (nM)	
			ScN2a cells	F3 cells
1,10-Phenanthroline			N.E.	N.E.
2,2',2''-Terpyridine			N.E.	N.E.
8-Hydroxyquinoline			N.E.	N.E.
Bis(8-quinolinolato) Copper(II)		Cu ²⁺	N.E.	N.E.
Bis(8-quinolinolato) Zinc(II)		Zn ²⁺	N.E.	N.E.
Neocuproine			80	N.E.
Bathocuproine			80	200
2,2'-Biquinoline			5	250
4,4'-Dicarboxy-2,2'-biquinoline			N.E.	N.E.

N.E., no effect.

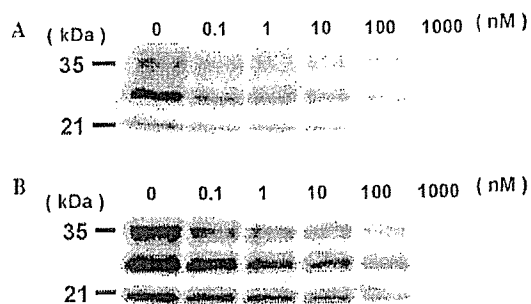
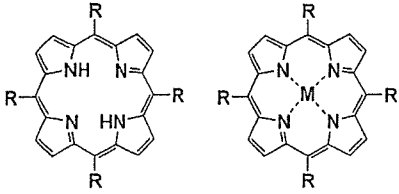
IC₅₀, concentration of a compound causing 50% inhibition of PrP-res formation relative to the control.

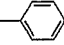
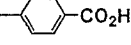
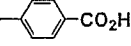
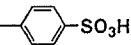
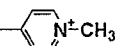
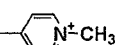
Figure 2. Anti-prion activity of 2,2'-biquinoline in prion-infected cells. Various concentrations of the compound were added to freshly passaged ScN2a cells (A) or F3 cells (B), and the PrP-res levels were analyzed by Western blotting. Lanes: 0, cells treated with DMSO alone; others, treated with the indicated concentration of 2,2'-biquinoline. Bars on the left indicate molecular mass markers at 35 and 21 kDa.

showed greater anti-prion activity than the metal-free compounds. Therefore, we examined whether SOD-like activity was associated with anti-prion activity, and discovered that this was the case.

PrP^C plays an important role in cell protection from oxidative stress, and modulates the activity of antioxidant enzymes by regulating the intracellular copper concentration, but it can also play a direct role owing to its intrinsic SOD activity.^{6,42,43} Cells with accumulated abnormal PrP^{Sc} displayed the phenotypes of decreased copper-binding capacity and higher sensitivity to oxidative stress.^{16,44} Interestingly, we found a significant correlation ($r = 0.93$) between SOD-like activity and anti-prion activity. Furthermore, we confirmed that the copper complex of D-penicillamine, which has been reported

Table 2. Inhibition of PrP-res formation in ScN2a cells and F3 cells by porphyrins



Compound	R	Metal(M)	Inhibition PrP-res	
			IC ₅₀ (nM)	
			ScN2a cells	F3 cells
TPP			10	320
TCPP			250	160
Mn-TCPP (MnTBAP)		Mn ³⁺	40	60
TPPS			200	160
TMPyP			130	160
Mn-TMPyP		Mn ³⁺	5	40

IC₅₀, concentration of a compound giving 50% inhibition of PrP-res formation relative to the control.

Table 3. SOD-like activity of metal complexes

Chelating metal	Compound	SOD-like activity IC ₅₀ (μM)
Cu	8-Hydroxyquinoline	263
	Clioquinol	140
	Neocuproine	50
	Bathocuproine	32
	2,2'-Biquinoline	3
	4,4'-Dicarboxy-2,2'-biquinoline	263
	Cimetidine	0.4
	D-Penicillamine	28
Mn	TCPP	8
	TMPyP	0.3
Fe	TPEN	0.4

IC₅₀, concentration of a compound giving 50% inhibition of WST-1 reduction.

to show anti-prion activity, exhibits SOD-like activity.¹³

It is not easy to find molecules with both good metal-binding ability and high SOD-like activity, because, taking copper ions as an example, the former property

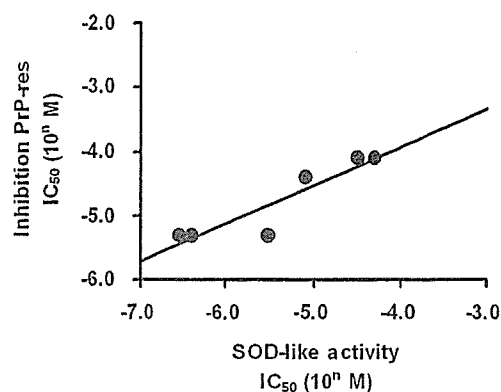


Figure 3. Correlation between SOD-like activity and inhibition of PrP-res formation in ScN2a cells. The plot shows data from seven compounds for which both SOD activity and inhibition of PrP-res formation were determined. ($r = 0.93$) SOD-like activity IC₅₀: concentration of a compound giving 50% inhibition of WST-1 reduction. Inhibition PrP-res IC₅₀: concentration of a compound giving 50% inhibition of PrP-res formation relative to the control.

means the Cu(II) complex is rather stable, while the latter property implies that the complex is prone to be reduced to the Cu(I)-chelator state.⁴⁵ This might explain why compounds such as clioquinol that are good copper chelators are nevertheless ineffective in terms of anti-prion activity.²⁵

On the other hand, cimetidine can form complexes with both Cu(I) and Cu(II), and has satisfactory SOD-like activity in both states, so it may be a good candidate for anti-prion activity. Furthermore, cimetidine can cross the blood-brain barrier to act in the central nerve system.⁴⁶ This type of compounds may provide a possible therapeutic approach for prion diseases.

In conclusion, we suggest that compounds which have copper-selective chelating ability, and whose copper complexes have high SOD-like activity are candidates for anti-prion drug.

References and notes

- Prusiner, S. B. *Science* **1982**, *216*, 136.
- Bounias, M.; Purdey, M. *Sci. Total Environ.* **2002**, *297*, 1.
- Brown, D. R.; Qin, K.; Herms, J. W.; Madlung, A.; Manson, J.; Strome, R.; Fraser, P. E.; Kruck, T.; von Bohlen, A.; Schulz-Schaeffer, W.; Giese, A.; Westaway, D.; Kretzschmar, H. *Nature* **1997**, *390*, 684.
- Viles, J. H.; Cohen, F. E.; Prusiner, S. B.; Goodin, D. B.; Wright, P. E.; Dyson, H. J. *Proc. Natl. Acad. Sci. U.S.A.* **1999**, *96*, 2042.
- Jackson, G. S.; Murray, I.; Hosszu, L. L.; Gibbs, N.; Waltho, J. P.; Clarke, A. R.; Collinge, J. *Proc. Natl. Acad. Sci. U.S.A.* **2001**, *98*, 8531.
- Brown, D. R.; Wong, B. S.; Hafiz, F.; Clive, C.; Haswell, S. J.; Jones, I. M. *Biochem. J.* **1999**, *344*, 1.
- Brown, D. R. *J. Neurosci. Res.* **1999**, *58*, 717.
- Pauly, P. C.; Harris, D. A. *J. Biol. Chem.* **1998**, *273*, 33107.

9. McKenzie, D.; Bartz, J.; Mirwald, J.; Olander, D.; Marsh, R.; Aiken, J. *J. Biol. Chem.* **1998**, *273*, 25545.
10. Brown, D. R.; Hafiz, F.; Glass-smith, L. L.; Wong, B. S.; Jones, I. M.; Clive, C.; Haswell, S. J. *EMBO J.* **2000**, *19*, 1180.
11. Kimberlin, R. H.; Millson, G. C.; Bountiff, L.; Collis, S. C. *J. Comp. Pathol.* **1974**, *84*, 263.
12. Pattison, I. H.; Jebbett, J. N. *Nature* **1971**, *230*, 115.
13. Sigurdsson, E. M.; Brown, D. R.; Alim, M. A.; Scholtzova, H.; Carp, R.; Meeker, H. C.; Prelli, F.; Frangione, B.; Wisniewski, T. *J. Biol. Chem.* **2003**, *278*, 46199.
14. Copper(II) perchlorate hexahydrate 98% and D-penicillamine were purchased from Sigma. Iron(II) sulfate heptahydrate, 2,2'-biquinoline, and cimetidine were purchased from Wako Pure Chemical (Osaka, Japan). 1,10-Phenanthroline monohydrate, 2,9-dimethyl-4,7-dimethyl-1,10-phenanthroline (bathocuproine), 2,9-1,10-phenanthroline (neocuproine), tetraphenylporphine (TPP), tetraphenylporphine tetrasulfonic acid (TPPS), $\alpha,\beta,\gamma,\delta$ -tetrakis(1-methylpyridinium-4-yl)porphine *p*-toluenesulfonate (TMPyP), tetrakis(4-carboxyphenyl)porphine (TCPP), 2,2'-bicinchoninic acid dipotassium salt, 5-chloro-7-iodo-8-hydroxyquinoline (clioquinol), and 8-hydroxyquinoline were purchased from Tokyo Kasei (Tokyo, Japan). Manganese(III) tetrakis(1-methylpyridinium-4-yl)porphyrin pentachloride (Mn-TMPyP) and Mn(III)tetrakis(4-benzoic acid)porphyrin chloride (Mn-TCPP or Mn-TBAP) were purchased from Calbiochem (California, USA). They were dissolved in 100% dimethylsulfoxide (DMSO) or 95% ethanol just before use.
15. Two types of prion-infected mouse neuroblastoma (N2a) cell lines were used in this study: N2a cells infected with the RML strain (ScN2a) [16] and N2a#58 cells infected with the Fukuoka-1 strain (F3). N2a#58 cells are known to express five times more normal PrP than N2a cells. Both ScN2a cells and F3 cells were grown in six-well culture plates in Opti-MEM (Invitrogen) supplemented with 10% fetal bovine serum. The cells were allowed to reach confluence, and chemicals at various concentrations were added to the medium when 5% of the confluent cells were passaged. The final concentration of either DMSO or ethanol in the medium was less than 0.2%. The cultures were allowed to grow to confluence (3 or 4 days).
16. Milhavet, O.; McMahon, H. E.; Rachidi, W.; Nishida, N.; Katamine, S.; Mange, A.; Arlotto, M.; Casanova, D.; Riondel, J.; Favier, A.; Lehmann, S. *Proc. Natl. Acad. Sci. U.S.A.* **2000**, *97*, 13937.
17. The chelation study was carried out using Job's method.^{18,19} Solutions of 10 mM Cu(II) and each compound at a compound:Cu (II) ratio of 1:0 to 0:1 were prepared in ultrapure water (MilliQ; Millipore Co., Japan) or 95% ethanol, and λ_{max} of the copper complex was measured.
18. Vosburgh, W. C.; Cooper, G. R. *J. Am. Chem. Soc.* **1941**, *63*, 437.
19. Job, P. *Ann. Chim.* **1928**, *9*, 113.
20. Kolthoff, I. M. S.; Sandell, E. B. *Textbook of Quantitative Inorganic Analysis*; Pergamon Press: New York, 1959, The MacMillan Co.
21. Ueno, K.; Imamura, T.; Cheng, K. L. *Handbook of Organic Analytical Reagents*; Pergamon Press: Tokyo, 1992, CRC Press.
22. Birker, P. J.; Freeman, H. C. *J. Am. Chem. Soc.* **1977**, *99*, 6890.
23. The anti-prion activity of each compound was assayed by measuring the 50%-inhibitory concentration (IC₅₀) for PrP-res formation in ScN2a cells and F3 cells, as described in previous reports.^{24–26} Briefly, compounds were added at designated concentrations to the medium when cells were passaged at 10% confluency. The cells were allowed to grow to confluence and lysed with lysis buffer (0.5% sodium deoxycholate, 0.5% Nonidet P-40, and PBS). The lysates were digested with 10 μ g/ml proteinase K for 30 min at 37 °C and centrifuged at 15,000 rpm for 5 min at 24 °C with GLASSFOG(Q-bio gene, USA). The pellets were resuspended in sample loading buffer and boiled. Samples were separated by electrophoresis on 15% Tris-glycine-SDS-polyacrylamide gel and electroblotted. PrP-res was detected using an antibody, SAF83 (1:5000; SPI-Bio, France), followed by an alkaline phosphatase-conjugated secondary antibody. Immunoreactive signals were visualized using CDP-Star detection reagent (Amersham Biosciences Corp., U.S.A.) and were analyzed densitometrically. At least three independent experiments were performed to estimate IC₅₀ of each compound.
24. Doh-Ura, K.; Iwaki, T.; Caughey, B. *J. Virol.* **2000**, *74*, 4894.
25. Murakami-Kubo, I.; Doh-ura, K.; Ishikawa, K.; Kawatake, S.; Sasaki, K.; Kira, J.; Ohta, S.; Iwaki, T. *J. Virol.* **2004**, *78*, 1281.
26. Ishikawa, K.; Doh-ura, K.; Kudo, Y.; Nishida, N.; Murakami-Kubo, I.; Ando, Y.; Sawada, T.; Iwaki, T. *J. Gen. Virol.* **2004**, *85*, 1785.
27. Day, B. J.; Shawen, S.; Liochev, S. I.; Crapo, J. D. *J. Pharmacol. Exp. Ther.* **1995**, *275*, 1227.
28. Day, B. J.; Crapo, J. D. *Toxicol. Appl. Pharmacol.* **1996**, *140*, 94.
29. Younes, M.; Lengfelder, E.; Zienau, S.; Weser, U. *Biochem. Biophys. Res. Commun.* **1978**, *81*, 576.
30. Kimura, E.; Sakonaka, A.; Nakamoto, M. *Biochim. Biophys. Acta* **1981**, *678*, 172.
31. Kimura, E.; Yatsunami, A.; Watanabe, A.; Machida, R.; Koike, T.; Fujioka, H.; Kuramoto, Y.; Sumomogi, M.; Kunimitsu, K.; Yamashita, A. *Biochim. Biophys. Acta* **1983**, *745*, 37.
32. Wada, K.; Fujibayashi, Y.; Yokoyama, A. *Arch. Biochem. Biophys.* **1994**, *310*, 1.
33. Goldstein, S.; Czapski, G. *Free Radic. Res. Commun.* **1991**, *12–13*, 205.
34. Baudry, M.; Etienne, S.; Bruce, A.; Palucki, M.; Jacobsen, E.; Malfroy, B. *Biochem. Biophys. Res. Commun.* **1993**, *192*, 964.
35. Darr, D. J.; Yanni, S.; Pinnell, S. R. *Free Radic. Biol. Med.* **1988**, *4*, 357.
36. Wada, K.; Fujibayashi, Y.; Tajima, N.; Yokoyama, A. *Biol. Pharm. Bull.* **1994**, *17*, 701.
37. SOD-like assay kit-WST (Dojindo Chemical, Kumamoto, Japan) was used for the quantification of SOD-like activity. This method is a xanthine-based spectrophotometric assay using the tetrazolium salt WST-1. The SOD-like activity was evaluated using the standard curve of SOD-like activity versus absorbance at 450 nm. Differences of SOD-like activity were tested by use of the unpaired Student's *t* test, and *p* values smaller than 0.05 were considered to be statistically significant.
38. Kimura, E.; Koike, T.; Shimizu, Y.; Kodama, M. *Inorg. Chem.* **1986**, *25*, 2242.
39. Nagano, T.; Hirano, T.; Hirobe, M. *J. Biol. Chem.* **1989**, *264*, 9243.
40. Hijazi, N.; Shaked, Y.; Rosenmann, H.; Ben-Hur, T.; Gabizon, R. *Brain Res.* **2003**, *993*, 192.
41. Cherny, R. A.; Atwood, C. S.; Xilinas, M. E.; Gray, D. N.; Jones, W. D.; McLean, C. A.; Barnham, K. J.; Volitakis, I.; Fraser, F. W.; Kim, Y.; Huang, X.; Goldstein, L. E.; Moir, R. D.; Lim, J. T.; Beyreuther, K.;

- Zheng, H.; Tanzi, R. E.; Masters, C. L.; Bush, A. I. *Neuron* **2001**, *30*, 665.
42. Martins, V. R.; Mercadante, A. F.; Cabral, A. L.; Freitas, A. R.; Castro, R. M. *Braz. J. Med. Biol. Res.* **2001**, *34*, 585.
43. Rachidi, W.; Vilette, D.; Guiraud, P.; Arlotto, M.; Riondel, J.; Laude, H.; Lehmann, S.; Favier, A. *J. Biol. Chem.* **2003**, *278*, 9064.
44. Rachidi, W.; Mange, A.; Senator, A.; Guiraud, P.; Riondel, J.; Benboubetra, M.; Favier, A.; Lehmann, S. *J. Biol. Chem.* **2003**, *278*, 14595.
45. Li, Q. X.; Luo, Q. H.; Li, Y. Z.; Shen, M. C. *Dalton Trans.* **2004**, 2329.
46. Totte, J.; Scharpe, S.; Verkerk, R.; Neels, H.; Vanhaeverbeek, M.; Smits, S.; Rousseau, J. J. *Lancet* **1981**, *1*, 1047.

Original Paper

Clusterin expression in follicular dendritic cells associated with prion protein accumulation

K Sasaki,^{1*} K Doh-ura,² JW Ironside,³ N Mabbott⁴ and T Iwaki¹

¹Department of Neuropathology, Neurological Institute, Graduate School of Medical Sciences, Kyushu University, Fukuoka 812-8582, Japan

²Division of Prion Biology, Department of Prion Research, CTAAR, Tohoku University School of Medicine, Sendai 980-8575, Japan

³National CJD Surveillance Unit, University of Edinburgh, Western General Hospital, Edinburgh EH4 2XU, UK

⁴Institute for Animal Health, Edinburgh EH9 3JF, UK

*Correspondence to:

Dr K Sasaki, Department of Neuropathology, Neurological Institute, Graduate School of Medical Sciences, Kyushu University, Fukuoka 812-8582, Japan.
E-mail: ksasaki@np.med.kyushu-u.ac.jp

Abstract

Peripheral accumulation of abnormal prion protein (PrP) in variant Creutzfeldt–Jakob disease and some animal models of transmissible spongiform encephalopathies (TSEs) may occur in the lymphoreticular system. Within the lymphoid tissues, abnormal PrP accumulation occurs on follicular dendritic cells (FDCs). Clusterin (apolipoprotein J) has been recognized as one of the molecules associated with PrP in TSEs, and clusterin expression is increased in the central nervous system where abnormal PrP deposition has occurred. We therefore examined peripheral clusterin expression in the context of PrP accumulation on FDCs in a range of human and experimental TSEs. PrP was detected immunohistochemically on tissue sections using a novel highly sensitive method involving detergent autoclaving pretreatment. A dendritic network pattern of clusterin immunoreactivity in lymphoid follicles was observed in association with the abnormal PrP on FDCs. The increased clusterin immunoreactivity appeared to correlate with the extent of PrP deposition, irrespective of the pathogen strains, host mouse strains or various immune modifications. The observed co-localization and correlative expression of these proteins suggested that clusterin might be directly associated with abnormal PrP. Indeed, clusterin immunoreactivity in association with PrP was retained after FDC depletion. Together these data suggest that clusterin may act as a chaperone-like molecule for PrP and play an important role in TSE pathogenesis. Copyright © 2006 Pathological Society of Great Britain and Ireland. Published by John Wiley & Sons, Ltd.

Received: 26 January 2006

Revised: 18 March 2006

Accepted: 28 March 2006

Keywords: prion; clusterin; follicular dendritic cell; immunohistochemistry; detergent autoclaving pretreatment; immune deficiency

Introduction

Transmissible spongiform encephalopathy (TSE) is the generic term for the fatal neurodegenerative diseases associated with abnormal prion protein (PrP) deposition in the central nervous system (CNS). Human TSE diseases include Creutzfeldt–Jakob disease (CJD), Gerstmann–Sträussler–Scheinker disease, fatal familial insomnia, and kuru. In cases of variant CJD, transmission is thought to have occurred from exposure to bovine spongiform encephalopathy (BSE)-contaminated meat via the oral route [1–3]. In cases of variant CJD and some animal TSE models, peripheral accumulation of abnormal PrP occurs in the lymphoreticular system, within the lymphoid follicles of spleens, lymph nodes, Peyer's patches, and tonsils [4–6]. In these regions, abnormal PrP accumulates on the surfaces of follicular dendritic cells (FDCs) from an early stage of the disease [7], followed by CNS involvement via the peripheral nervous system [8,9].

Clusterin (apolipoprotein J) is a heterodimeric glycoprotein and is expressed in a variety of mammalian tissues. It is considered to have a variety of functions,

including inhibition of complement-mediated cytotoxicity by binding to the membrane attack complex [10]; regulation of apoptosis [11]; and as a survival factor for germinal centre B cells [12]. We have reported that, during TSE disease, clusterin is associated with deposits of abnormal PrP in the CNS [13]. In the CNS of TSE-affected subjects, clusterin co-localizes with the extracellular plaque-type PrP deposits. Clusterin expression is also up-regulated within lesions of synaptic PrP deposition, even though no co-localization is observed. As clusterin interacts with a range of other molecules [14,15], these findings suggest that secreted clusterin might act as a chaperone-like molecule for PrP. Previous *in vitro* investigations have shown that clusterin is induced in astrocytes by PrP fragments reminiscent of the abnormal PrP isoform [16], and prevents their fibrillar aggregation [17].

FDCs also express clusterin [12]. Therefore we investigated whether clusterin expression in the lymphoreticular system is likewise affected by TSE infection, and associated with the extracellular accumulation of abnormal PrP on FDCs.

Materials and methods

Antibodies

The antibodies used included anti-human PrP C-terminal (rabbit polyclonal, IBL, Japan; raised against a peptide mapping to the C-terminus of human PrP, cross-reacts with mouse PrP), anti-human PrP N-terminal (rabbit, IBL; raised against a peptide mapping to the N-terminus of human PrP, cross-reacts with mouse PrP), anti-human PrP (mouse monoclonal, 3F4, Signet, MA, USA; recognizing amino acid residues 109–112, cross-reacts with hamster PrP), anti-mouse clusterin (goat polyclonal, M-18, Santa Cruz, CA, USA; raised against a peptide mapping to the C-terminus of mouse clusterin), anti-human clusterin (goat, C-18, Santa Cruz; raised against a peptide mapping to the C-terminus of human clusterin), or anti-human clusterin (goat, Chemicon, CA, USA; raised against a purified clusterin from human plasma), anti-mouse CD21/CD35 (CR2/CR1, rat monoclonal, 7G6, PharMingen, CA, USA), anti-human CD35 (CR1, mouse, Ber-MAC-DRC, Dako, Denmark). We assessed two anti-human clusterin antibodies by immunohistochemistry and verified that both gave similar results [13].

Mouse models

Non-transgenic NZW mice and transgenic Tga20 mice [18,19] that express high amounts of mouse PrP were inoculated intraperitoneally (i.p.) with the Fukuoka-1 mouse-passaged scrapie agent strain (NZW/Fu-1, Tga20/Fu-1, respectively). Transgenic Tg7 mice [8,20] that express high amounts of hamster PrP on a mouse-PrP knockout background were inoculated i.p. with the 263K hamster-passaged scrapie agent strain (Tg7/263K). Permission for these animal experiments was obtained from the Animal Experiment Committee of Kyushu University.

Where indicated, C57BL/Dk mice were inoculated either orally or i.p. with the ME7 mouse-passaged

scrapie agent strain (C57BL/ME7 mice). To deplete FDCs temporarily, C57BL/Dk mice were given a single i.p. injection of a fusion protein containing the soluble lymphotoxin β receptor domain linked to the Fc portion of human IgG1 (LT β R-Ig) or 100 μ g polyclonal human IgG (hu-Ig) (Sandoglobulin[®]) as a control [21,22]. Where indicated, treatment was given 3 days before (–3 dpi) oral inoculation, or 14 or 42 days after (14 dpi & 42 dpi, respectively) i.p. inoculation with the ME7 scrapie agent strain as described [21,22]. Spleens were analysed 3 days after treatment; Peyer's patches were analysed 70 days after inoculation with the scrapie agent. Mice deficient in interleukin-6 (IL-6-knockout (KO) mice, on a 129/Sv \times C57BL/6 background) possess FDC networks but have impaired germinal centres [23]. IL-6-KO mice, and 129/Sv \times C57BL/6 immunocompetent wild-type mice, were also inoculated i.p. with the ME7 mouse-passaged scrapie agent strain. Permission for these animal experiments was obtained from the Ethical Review Committee at the Institute for Animal Health, Edinburgh, UK.

Table 1 summarizes the profiles of the mouse lines used in this study.

Human CJD cases

Paraffin-embedded sections of spleens, lymph nodes, appendices, and tonsils were examined from five cases of variant CJD (three males, two females, age range 17–39 years, duration of clinical illness 7–33 months) from the UK National CJD Surveillance Unit, University of Edinburgh, UK. Spleen sections were also examined from four cases of sporadic CJD (two males, two females, age range 55–69 years, duration of clinical illness 4–30 months) from the Department of Neuropathology, Kyushu University. The diagnosis of variant or sporadic CJD was confirmed by postmortem examination. Each case had consent for use of autopsy tissues for research purposes and local Ethics Committee approval for the use of human autopsy tissues from patients with CJD for research was also obtained.

Table 1. Profiles of mouse lines

Line	Background	Modification of PrP expression	PrP ^c on FDCs	Reference	Inoculum	PrP ^{sc} on FDCs
NZW wild		None	+		Fukuoka-1	+
C57BL/Dk Wild		None	+		ME7	+
Tg7	C57BL/10	MoPrP knockout Overexpress HaPrP under control of the endogenous MoPrP promoter	+	8,20	263K	–
Tga20	129/Sv \times C57BL/6	MoPrP knockout Overexpress MoPrP under control of the endogenous MoPrP promoter	–*	18,19	Fukuoka-1	–
IL-6 KO	129/Sv \times C57BL/6	None	+	23	ME7	+

MoPrP = mouse PrP; HaPrP = hamster PrP; PrP^c = cellular PrP expression on the FDCs; PrP^{sc} = abnormal PrP accumulation on FDCs of scrapie affected mice; (–) negative; (+) positive.

* Negative on FDCs but some cells within the paracortical T-cell area express PrP^c [19].

The inocula indicated were applied to the respective mouse lines in this study.

Immunohistochemistry

To enhance the detection of PrP by immunohistochemistry (IHC), formalin-fixed, paraffin-embedded sections were pretreated by hydrolytic autoclaving (1–2 mM HCl, 121 °C, 10 min) or a protocol using formic acid, guanidine thiocyanate, and hydrated autoclaving as previously reported [24,25]. We also performed an autoclaving pretreatment with Target Retrieval Solution (Dako) or buffer solution with detergent. A variety of detergents were examined including, Triton X-100 and Tween-20 as non-ionic detergents and sodium dodecyl sulphate as an ionic detergent. We found that non-ionic detergents enhanced PrP detection to a similar degree, whereas the ionic detergent enhanced PrP detection sensitivity, but caused considerable tissue damage. Autoclaving the sections in 0.1% Triton X-100 in 50 mM Tris-HCl, pH 7.6, 121 °C, 20 min, was found to be the most suitable method for the detection of abnormal PrP accumulation on FDCs, and was used in this study (hereinafter referred to as the detergent autoclaving method). Increased concentrations of Triton X-100 up to 0.5% did not significantly increase the signal intensity of the PrP detected or affect the degree of tissue damage. This indicated that the detergent autoclaving method had a wider range of optimum detergent concentrations than the HCl in the hydrolytic autoclaving method. Immunoreactions were visualized using diaminobenzidine as a chromogen.

To examine the co-localization of two different proteins on the same section, the first immunoreaction was visualized using 3-amino-9-ethylcarbazole (AEC; Vector, CA, USA), mapped, and photographed. The section was then decolourized by immersing it in ethanol, and the second immunohistochemical procedure was

performed with the other primary antibody. Double immunofluorescence was also performed to reveal sites of co-localization.

Results

Experiments demonstrated that the detergent autoclaving method was the most useful for detecting PrP by IHC. This was particularly evident on sections of spleen tissue, where this method drastically improved the signal intensity for PrP accumulated on FDCs in comparison with sections treated by the HCl autoclave method (Figure 1A and B, respectively). Table 2 shows comparisons between this detergent autoclaving method and conventional techniques for IHC detection of PrP. On human brain samples, most of the different types of PrP deposition could be detected by the detergent autoclaving method as well as by conventional techniques (Figure 1C and 1D, respectively). However, the detergent autoclaving method

Table 2. Comparison of the methods of immunohistochemistry for PrP

	Detergent autoclaving	HCl autoclaving [24]	Three steps [25]
PrP signal intensity			
Synaptic	+ ~ ++	++	+ ~ ++
Plaque	++	++	++
FDCs (mouse)	++	+	++
Background	Low	High	Moderate
Tissue damage	Low	High	Moderate
Simplicity	Simple	Moderate	Complicated

(+) positive; (++) strongly positive. In the three steps method samples are pretreated with formic acid, guanidine thiocyanate, and hydrated autoclaving.

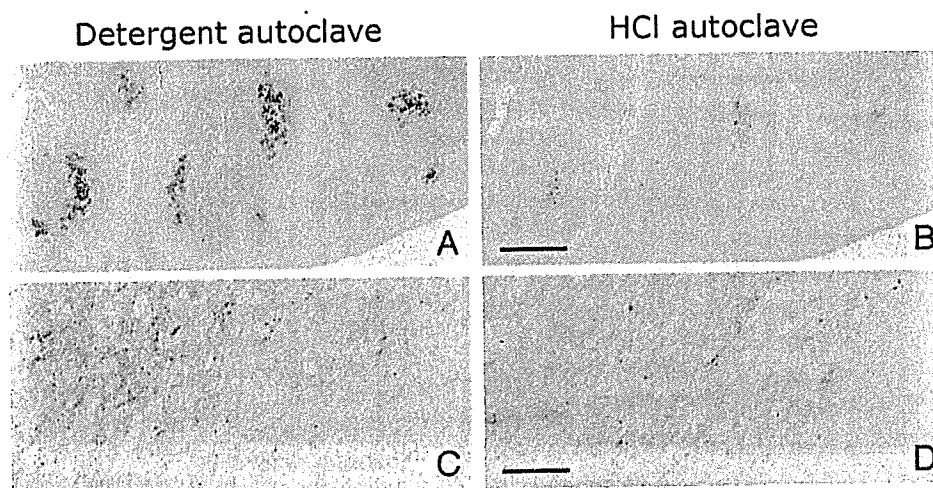


Figure 1. Effect of detergent autoclaving pretreatment on the detection of PrP by immunohistochemistry. (A, B) Serial sections of spleen from TSE-infected mice (NZW mouse inoculated with Fukuoka-1 strain) were immunostained for PrP. The detergent autoclaving method (A) dramatically increased the signal intensity of the PrP immunoreaction and lowered non-specific background staining in comparison with the HCl autoclaving method (B). (C, D) Serial sections of cerebral cortex from a case with sporadic CJD immunostained for PrP. Immunoreactivity for PrP is rather weak on sections pretreated by the detergent autoclaving method (C) in comparison with those pretreated by the HCl autoclaving method (D). However, abnormal fine granular deposits of PrP are detected by both methods. Bars: 200 μ m (A, B), 100 μ m (C, D)

decreased background staining, which facilitated the double immunofluorescence technique in this study.

We examined the lymphoreticular system of mouse models of TSE. In the spleens of scrapie agent-inoculated NZW/Fu-1 ($n = 5$) and C57BL/ME7 mice ($n = 3$), abnormal PrP accumulated on the dendritic network of FDCs as the disease progressed (Figure 2E), but not in the spleens of uninoculated NZW mice ($n = 5$) (Figure 2B) or scrapie agent-inoculated Tg7/263K ($n = 5$) or Tga20/Fu-1 mice ($n = 3$)(data not shown). The apparent lack of cellular

PrP expression by FDCs in the spleens of Tga20 mice probably prevents abnormal PrP amplification on these cells [19]. Likewise, after high-dose scrapie inoculation into these transgenic mice, neuroinvasion probably occurs via a putative 'direct neuroinvasion' pathway without the need for prior amplification of abnormal PrP on FDCs [8]. In uninoculated NZW mice, clusterin was constitutively and diffusely expressed in the reticular cells in lymphoid follicles (Figure 2A), as previously reported [26]. However, in the spleens of NZW/Fu-1 mice immunoreactivity for clusterin was

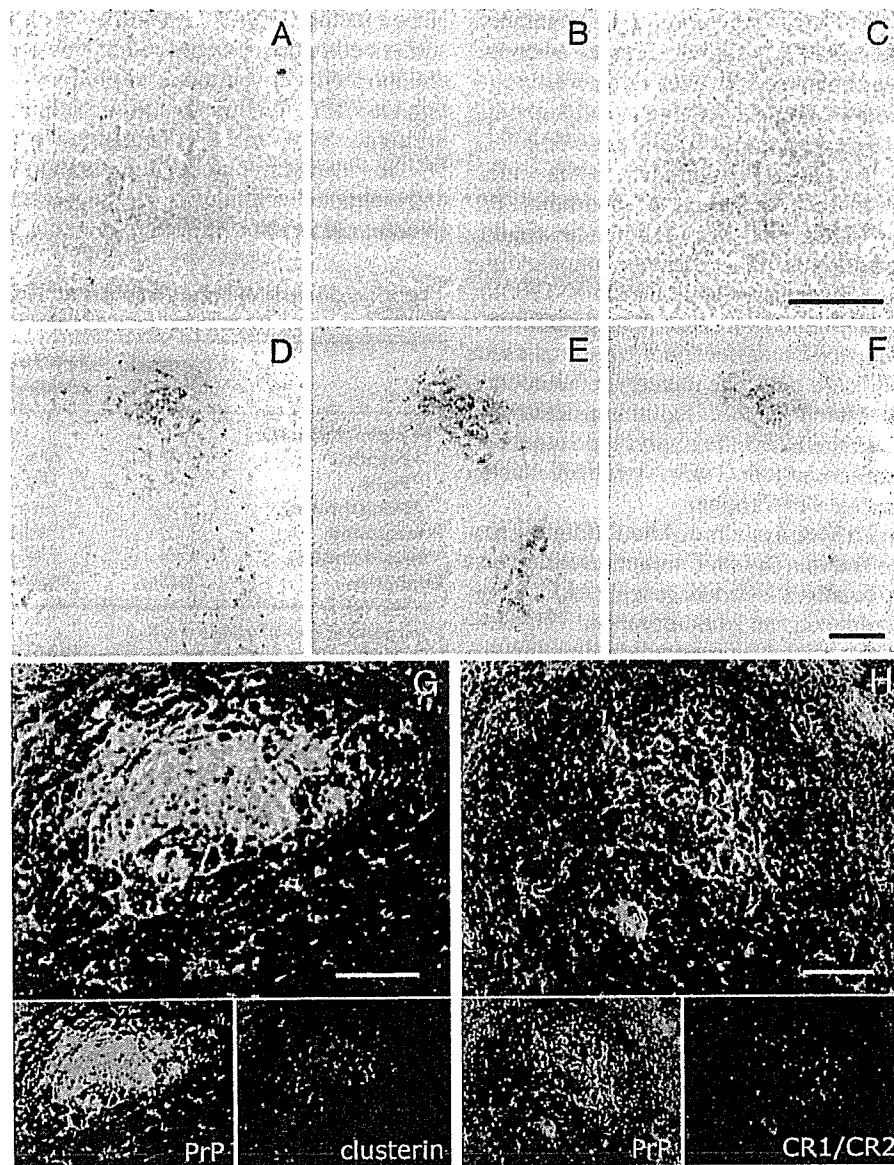


Figure 2. Immunohistochemistry for clusterin expression on FDCs in the spleens of uninoculated and scrapie-inoculated mice. (A–C) Serial sections of uninoculated NZW mouse spleen were immunostained for clusterin (A), PrP (B), and CR1/CR2 (C). Clusterin is constitutively expressed in the reticular cells in the lymphoid follicles of uninoculated mice (A) and not obviously condensed on the dendritic network of FDCs (C). However, increased clusterin expression was observed on FDCs from scrapie-inoculated mice. (D–F) The same section of spleen from the NZW/Fu-1 TSE mouse model was serially immunostained for clusterin (D), PrP (E), and CR1/CR2 (F). Immunoreactivity for clusterin is markedly condensed and increased on the FDCs associated with abnormal PrP accumulation. Similar results were observed in the C57BL/ME7 mouse model. The co-localization of these proteins was also confirmed by double immunofluorescence (G, H). (G) Clusterin (red) and PrP (green). (H) CR1/CR2 (red) and PrP (green). Bars: 100 μm (A–F), 50 μm (G, H)

condensed (Figure 2D) and co-localized with the PrP (Figure 2E) accumulated on the complement receptor 1/2 (CR1/CR2)-immunopositive dendrites [27] of FDCs (Figure 2F). No such accentuation of clusterin expression was observed in the spleens of scrapie-inoculated Tg7/263K mice or Tga20/Fu-1 mice (data not shown). The co-localization of clusterin and PrP on the FDCs was also confirmed by double immunofluorescence (Figure 2G and H).

Although the increased clusterin immunoreactivity mostly correlated with the abnormal PrP accumulations on splenic FDCs from scrapie-agent inoculated C57BL/ME7 mice, temporary FDC depletion 14 or 42 days after scrapie-agent inoculation [21,22] did not affect the association of clusterin with abnormal PrP (Table 3). Similarly, in the spleens of scrapie agent-inoculated IL-6-KO mice, immunoreactivity for clusterin was mostly correlated with abnormal PrP accumulation (Table 3) despite the impaired germinal centre development in these mice [23].

In Peyer's patches, increased clusterin expression was seen not only on the PrP-immunopositive FDCs of infected mice but also in the lymphoid follicles without PrP deposition (Table 3). Clusterin-labelled lymphoid follicles were also confirmed in the Peyer's patches of non-infected control mice (data not shown), but this occurred to a lesser extent than in TSE-infected mice.

Increased clusterin expression associated with the abnormal PrP deposition on FDCs was also observed in cases of human variant CJD. The extent and

intensity of clusterin immunoreactivity did not appear to be related to the age of the patient, or the duration of the clinical illness of the five cases examined (patient ages 17, 29, 33, 36, and 39 years; duration of clinical illness 33, 7, 18, 15, and 14 months, respectively). In each case, immunoreactivity for clusterin was increased wherever abnormal PrP accumulation on the FDCs was found, such as in the spleens, lymph nodes, appendices, and tonsils (Figure 3). In appendices, clusterin immunoreactivity was also increased in the lymphoid follicles without PrP deposition (Figure 3C and D), which was consistent with data from analysis of Peyer's patches of mouse TSE models. No increased clusterin immunoreactivity was observed on FDCs from sporadic CJD cases (data not shown) in which no PrP deposition was detected, except on appendices where clusterin immunoreactivity was increased on the FDCs even in non-CJD control cases (Figure 3E and F).

Discussion

Here we show that clusterin expression on FDCs is increased during TSE diseases and occurs in association with abnormal PrP accumulation. The dendritic network pattern of the clusterin immunoreactivity in the lymphoid follicles was associated with PrP accumulation on FDCs in NZW/Fu-1 mice and C57BL/ME7 mice. The increased clusterin immunoreactivity was mostly dependent on the presence of

Table 3. Effect of FDC depletion and impaired germinal centre development on clusterin expression in TSE-inoculated mice

	Immune deficiency	PrP IR	Clusterin IR*	CR1/CR2 IR	Effect on disease transmission†
Intraperitoneal					
Spleens					
Uninfected					
LT β R-Ig	FDCs depleted	–	–	–	n/a
Hu-Ig	Control	–	–	+	n/a
14 dpi					
LT β R-Ig	FDCs depleted	–	–	–	Delayed [21]
Hu-Ig	Control	+–	–	+	
42 dpi					
LT β R-Ig	FDCs depleted	+	+	–	Delayed [21]
Hu-Ig	Control	+	+	++	
IL-6-KO					
	Impaired germinal centres	++	+	++	No effect [23]
Wild-type	Control	++	+	++	
Oral					
Peyer's patches					
–3 dpi					
LT β R-Ig	FDCs depleted	–	+‡	n.d.	Inhibited [22]
Hu-Ig	Control	+	+‡	n.d.	

FDCs were depleted by treatment with LT β R-Ig, or Hu-Ig as a control [28]. Ig treatment was performed on the indicated days relative to scrapie challenge. Three mice were examined and estimated the immunoreactivity on each immune-deficient group (LT β R-Ig treated or IL-6 KO) or control group.

IR = immunoreactivity; dpi = days post scrapie inoculation; n.d. = not determined; n/a = not applicable; (–) = negative; (+–) = faint; (+) = positive; (++) = strongly positive.

* Immunoreactivity in the dendritic-network pattern.

† Data from previous reports [21–23].

‡ Clusterin immunoreactivity does not always correlate with PrP deposition; increased clusterin expression is also seen in some lymphoid follicles without PrP accumulation.

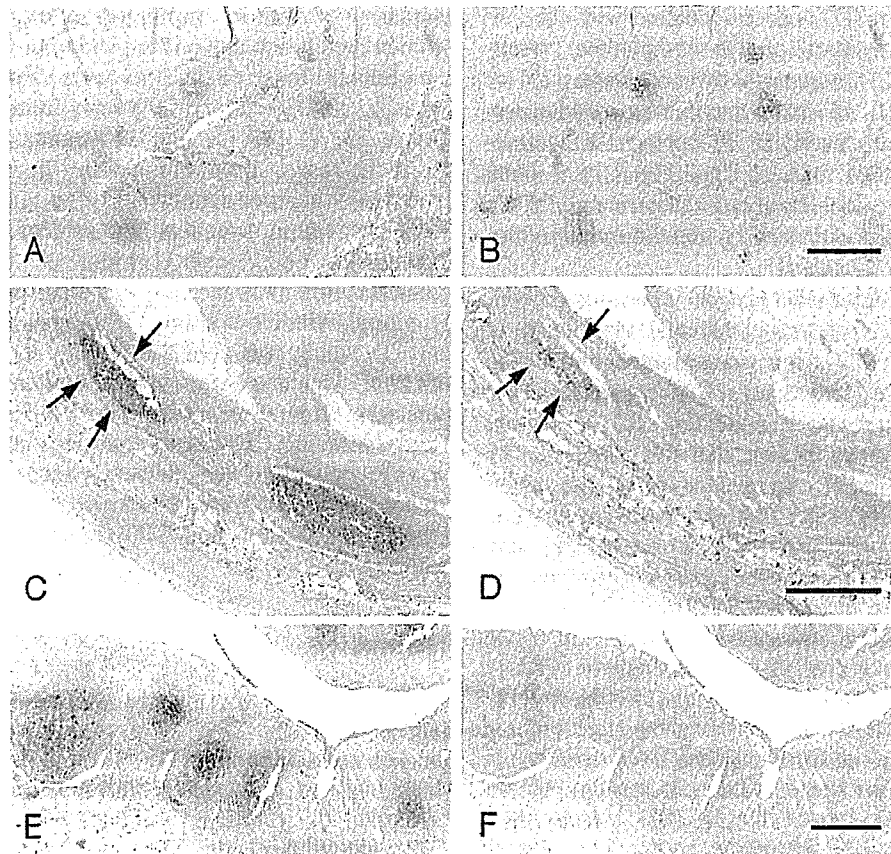


Figure 3. Immunohistochemistry of lymphoreticular tissues from human variant CJD and control (non-CJD) cases. (A, C, E) Clusterin. (B, D, F) PrP. (A, B) Serial sections of the tonsil from a variant CJD case. Clusterin immunoreactivity is increased on FDCs where abnormal PrP deposits are detected. (C–F) Serial sections of appendices from a variant CJD case (C, D) and a control case (E, F). Note that not only the lymphoid follicles with PrP accumulation (arrows) but also those without PrP accumulation show increased clusterin expression. Bars: 500 μ m

abnormal PrP deposition, irrespective of the TSE agent strains, host mouse strains, or various immune deficiencies. Moreover, clusterin accumulation was also seen in human variant CJD cases, which was consistently accompanied by PrP deposition on FDCs in the lymphoreticular system (except for the intestinal lymphoid follicles). We have previously reported that clusterin expression in the cerebrum was increased in association with increased PrP deposition [13]. The results in the present report provide evidence that clusterin accumulation also occurs in peripheral lymphoid tissues. Although a direct interaction between clusterin and PrP remains to be confirmed, these data suggest that clusterin may play an important role in the pathogenesis of TSE diseases in lymphoid tissues.

To determine whether clusterin was associated with abnormal PrP, we analysed the effect of FDC depletion on clusterin accumulation. Signalling through the $LT\beta R$ provides important stimuli for FDC maturation and maintenance. Blockade of this stimulation through treatment with $LT\beta R$ -Ig causes the temporary de-differentiation of FDCs [28]. In this study, CR1/CR2 expression on FDCs was certainly affected by $LT\beta R$ -Ig treatment in comparison with the control mice treated with Hu-Ig (Table 3), confirming that the

FDCs were temporarily de-differentiated. In uninoculated mice, clusterin expression by FDCs is down-regulated by $LT\beta R$ signalling blockade and undetectable by immunohistochemistry within two days of FDC depletion [12]. However, in this study we show that the detection of clusterin in the spleens of scrapie-inoculated mice was unaffected by FDC depletion and remained in close association with abnormal PrP (Table 3). These data imply that clusterin associates directly with abnormal PrP molecules exposed extracellularly on the surface of FDC dendrites.

Why clusterin expression is up-regulated during TSE disease is not known. Data from both human and experimental studies demonstrate that TSE infections induce the expression of both early and terminal complement components within the brain. However, the membrane attack complex (C5b–C9) is not involved in TSE pathogenesis [29]. Thus it is plausible that, during TSE diseases within the CNS, clusterin might be expressed as part of an innate response to inactivate the membrane attack complex formed by the terminal complement components [10], and to help protect neurons from potential complement-mediated lysis. It is also plausible that clusterin might be induced to exert anti-amyloidogenic properties [30]. Because

FDCs express clusterin (current study and reference [12]), and its expression appears to be up-regulated during TSE disease, it is plausible that clusterin is likewise released by FDCs as an activating factor for themselves and/or neighbouring germinal centre B cells [12], which might accelerate abnormal PrP accumulation.

In the Peyer's patches and appendices, some lymphoid follicles showed no detectable PrP deposition, but revealed enhanced clusterin immunoreactivity. Although it is possible that small amounts of undetectable abnormal PrP molecules were present in these follicles, enhanced clusterin expression at this site was probably due to non-specific immune stimulation. Clusterin-enhanced lymphoid follicles were confirmed even in the Peyer's patches of non-infected control mice and in the appendices of non-CJD control cases. The continual exposure of the intestinal lymphoreticular system to a variety of antigens or stress conditions might account for the enhanced clusterin expression in non-TSE affected subjects in comparison with the spleens. The reasons why the regulation of clusterin expression on FDCs in the intestine and other lymphoid tissues appears to differ in uninfected hosts are unknown and therefore worthy of further investigation.

We employed a detergent autoclaving method for PrP detection in this study and found that this method significantly improved sensitivity, especially when analysing the lymphoreticular pathology of TSEs. The early detection of PrP accumulation on FDCs might aid the detection of scrapie transmissibility, and the diagnosis of human variant CJD, for example on tonsil biopsy specimens. Detergent autoclaving also provides a less harsh pretreatment for antigen retrieval, avoids tissue damage, and reduces non-specific background staining. Prolonged formalin fixation of tissue samples results in a considerable reduction of PrP immunoreactivity. This effect might be overcome by modifying the concentration of detergents and/or autoclaving time without causing significant tissue damage.

In conclusion, we have demonstrated that clusterin expression was increased in association with abnormal PrP deposits not only in the CNS [13] but also in the peripheral lymphoreticular system. The observed co-localization and correlative expression of these proteins implies that clusterin might have an important role in PrP pathogenesis in the TSEs, perhaps as a chaperone-like molecule. In keeping with this suggestion, Kempster and associates reported that clusterin-deficient mice inoculated i.p. with mouse-passaged BSE agent had an increased incubation time in comparison with wild-type mice [31]. Thus clusterin might influence the accumulation and/or aggregation of PrP on FDCs, and affect disease progression. Comparative transmission studies using clusterin-deficient mice inoculated with a variety of TSE agent strains by various peripheral routes of exposure will provide further insights into the role of clusterin in TSE pathogenesis.

Acknowledgements

This work was supported by grants to K Doh-ura and T Iwaki from the Ministry of Health, Labour and Welfare, Japan and a grant to K Sasaki from the Japan Society for the Promotion of Science. We thank Ms K Hatanaka, Ms S Nagae, and Mr S Mawatari for their excellent technical assistance. Part of this study was carried out at the Morphology Core, Graduate School of Medical Sciences, Kyushu University. LT β R-Ig and Hu-Ig were kindly provided by Dr Jeffrey Browning (Biogen Inc, Cambridge, MA, USA) and requests for these reagents should be addressed to Jeff.Browning@biogen.com.

References

- Collinge J, Sidle KC, Meads J, Ironside J, Hill AF. Molecular analysis of prion strain variation and the aetiology of 'new variant' CJD. *Nature* 1996;**383**:685–690.
- Bruce ME, Will RG, Ironside JW, McConnell I, Drummond D, Suttie A, et al. Transmissions to mice indicate that 'new variant' CJD is caused by the BSE agent. *Nature* 1997;**389**:498–501.
- Hill AF, Desbruslais M, Joiner S, Sidle KC, Gowland I, Collinge J, et al. The same prion strain causes vCJD and BSE. *Nature* 1997;**389**:448–450, 526.
- Hill AF, Zeidler M, Ironside J, Collinge J. Diagnosis of new variant Creutzfeldt-Jakob disease by tonsil biopsy. *Lancet* 1997;**349**:99–100.
- Kitamoto T, Muramoto T, Mohri S, Doh-Ura K, Tateishi J. Abnormal isoform of prion protein accumulates in follicular dendritic cells in mice with Creutzfeldt-Jakob disease. *J Virol* 1991;**65**:6292–6295.
- van Keulen LJ, Schreuder BE, Meloen RH, Mooij-Harkes G, Vromans ME, Langeveld JP. Immunohistochemical detection of prion protein in lymphoid tissues of sheep with natural scrapie. *J Clin Microbiol* 1996;**34**:1228–1231.
- Jeffrey M, McGovern G, Goodsir CM, Brown KL, Bruce ME. Sites of prion protein accumulation in scrapie-infected mouse spleen revealed by immuno-electron microscopy. *J Pathol* 2000;**191**:323–332.
- Race R, Oldstone M, Chesebro B. Entry versus blockade of brain infection following oral or intraperitoneal scrapie administration: role of prion protein expression in peripheral nerves and spleen. *J Virol* 2000;**74**:828–833.
- Glatzel M, Heppner FL, Albers KM, Aguzzi A. Sympathetic innervation of lymphoreticular organs is rate limiting for prion neuroinvasion. *Neuron* 2001;**31**:25–34.
- Schopp J, Chonn A, Hertig S, French LE. Clusterin, the human apolipoprotein and complement inhibitor, binds to complement C7, C8-beta, and the b domain of C9. *J Immunol* 1993;**151**:2159–2165.
- French LE, Wohlwend A, Sappino AP, Tschopp J, Schifferli JA. Human clusterin gene expression is confined to surviving cells during in vitro programmed cell death. *J Clin Invest* 1994;**93**:877–884.
- Huber C, Thielen C, Seeger H, Schwarz P, Montrasio F, Wilson MR, et al. Lymphotoxin-beta receptor-dependent genes in lymph node and follicular dendritic cell transcriptomes. *J Immunol* 2005;**174**:5526–5536.
- Sasaki K, Doh-ura K, Ironside JW, Iwaki T. Increased clusterin (apolipoprotein J) expression in human and mouse brains infected with transmissible spongiform encephalopathies. *Acta Neuropathol (Berl)* 2002;**103**:199–208.
- Wilson MR, Easterbrook-Smith SB. Clusterin is a secreted mammalian chaperone. *Trends Biochem Sci* 2000;**25**:95–98.
- Sasaki K, Doh-ura K, Wakisaka Y, Iwaki T. Clusterin/apolipoprotein J is associated with cortical Lewy bodies: immunohistochemical study in cases with alpha-synucleinopathies. *Acta Neuropathol (Berl)* 2002;**104**:225–230.
- Chiesa R, Angeretti N, Lucca E, Salmona M, Tagliavini F, Bugiani O, et al. Clusterin (SGP-2) induction in rat astroglial

- cells exposed to prion protein fragment 106–126. *Eur J Neurosci* 1996;**8**:589–597.
17. McHattie S, Edington N. Clusterin prevents aggregation of neuropeptide 106–126 in vitro. *Biochem Biophys Res Commun* 1999;**259**:336–340.
 18. Fischer M, Rulicke T, Raeber A, Sailer A, Moser M, Oesch B, *et al.* Prion protein (PrP) with amino-proximal deletions restoring susceptibility of PrP knockout mice to scrapie. *EMBO J* 1996;**15**:1255–1264.
 19. Thackray AM, Klein MA, Bujdoso R. Subclinical prion disease induced by oral inoculation. *J Virol* 2003;**77**:7991–7998.
 20. Race RE, Priola SA, Bessen RA, Ernst D, Dockter J, Rall GF, *et al.* Neuron-specific expression of a hamster prion protein minigene in transgenic mice induces susceptibility to hamster scrapie agent. *Neuron* 1995;**15**:1183–1191.
 21. Mabbott NA, Mackay F, Minns F, Bruce ME. Temporary inactivation of follicular dendritic cells delays neuroinvasion of scrapie. *Nat Med* 2000;**6**:719–720.
 22. Mabbott NA, Young J, McConnell I, Bruce ME. Follicular dendritic cell dedifferentiation by treatment with an inhibitor of the lymphotoxin pathway dramatically reduces scrapie susceptibility. *J Virol* 2003;**77**:6845–6854.
 23. Mabbott NA, Williams A, Farquhar CF, Pasparakis M, Kollias G, Bruce ME. Tumor necrosis factor alpha-deficient, but not interleukin-6-deficient, mice resist peripheral infection with scrapie. *J Virol* 2000;**74**:3338–3344.
 24. Kitamoto T, Shin RW, Doh-ura K, Tomokane N, Miyazono M, Muramoto T, *et al.* Abnormal isoform of prion proteins accumulates in the synaptic structures of the central nervous system in patients with Creutzfeldt-Jakob disease. *Am J Pathol* 1992;**140**:1285–1294.
 25. Bell JE, Gentleman SM, Ironside JW, McCardle L, Lantos PL, Doey L, *et al.* Prion protein immunocytochemistry — UK five centre consensus report. *Neuropathol Appl Neurobiol* 1997;**23**:26–35.
 26. Wellmann A, Thieblemont C, Pittaluga S, Sakai A, Jaffe ES, Siebert P, *et al.* Detection of differentially expressed genes in lymphomas using cDNA arrays: identification of clusterin as a new diagnostic marker for anaplastic large-cell lymphomas. *Blood* 2000;**96**:398–404.
 27. Whipple EC, Shanahan RS, Ditto AH, Taylor RP, Lindorfer MA. Analyses of the in vivo trafficking of stoichiometric doses of an anti-complement receptor 1/2 monoclonal antibody infused intravenously in mice. *J Immunol* 2004;**173**:2297–2306.
 28. Mackay F, Browning JL. Turning off follicular dendritic cells. *Nature* 1998;**395**:26–27.
 29. Mabbott NA, Bruce ME. Complement component C5 is not involved in scrapie pathogenesis. *Immunobiology* 2004;**209**:545–549.
 30. Zlokovic BV. Cerebrovascular transport of Alzheimer's amyloid beta and apolipoproteins J and E: possible anti-amyloidogenic role of the blood-brain barrier. *Life Sci* 1996;**59**:1483–1497.
 31. Kempster S, Collins ME, Aronow BJ, Simmons M, Green RB, Edington N. Clusterin shortens the incubation and alters the histopathology of bovine spongiform encephalopathy in mice. *Neuroreport* 2004;**15**:1735–1738.

Case Report

Increased asymmetric pulvinar magnetic resonance imaging signals in Creutzfeldt–Jakob disease with florid plaques following a cadaveric dura mater graft

Yoshinobu Wakisaka,^{1,2} Naohiko Santa,^{2,3} Katsumi Doh-ura,⁴ Tetsuyuki Kitamoto,⁴ Setsuro Ibayashi,² Mitsuo Iida² and Toru Iwaki¹

¹Department of Neuropathology, Neurological Institute, and ²Department of Medicine and Clinical Science, Graduate School of Medical Sciences, Kyushu University, Fukuoka, ³Cerebrovascular Department, Neuroscience Institute, St Mary Hospital, Kurume, and ⁴Department of Prion Research, Tohoku University Graduate School of Medicine, Sendai, Japan

A 9-year-old Japanese girl received a cadaveric dura mater graft during surgery following a head injury with brain contusion. She continued to do well, but when she became 19-years-old, she gradually showed a violent character and was treated in a psychiatric hospital. Another 6 years later, 200 months after the procedure, she developed a progressive gait ataxia, which subsequently led to her death within 10 months of onset. An autopsy showed she had CJD. This patient represents an atypical case of dura-associated CJD (dCJD) with unusual clinicopathological features including the late occurrence of myoclonus, an absence of periodic synchronous discharges in the electroencephalogram, and the presence of widespread florid plaques. However, our detection of an asymmetrical increase in the MRI-derived images of pulvinar nuclei has not been previously observed in other atypical cases of dCJD. Because atypical dCJD cases share several clinicopathological features with those of vCJD, and because asymmetrical hyperintense signals in the pulvinar have been observed in some neuropathologically confirmed vCJD cases, we had some difficulty in a differential diagnosis between atypical dCJD and vCJD. This is the first atypical dCJD case showing a pulvinar high signal compared with all other basal ganglia on MRI.

Key words: CJD, dura graft, MRI, pulvinar sign, vCJD.

Correspondence: Dr Yoshinobu Wakisaka, MD, PhD, Department of Medicine and Clinical Science, Graduate School of Medical Sciences, Kyushu University, 3-1-1 Maidashi, Higashi-ku, Fukuoka, 812-8582, Japan. Email: w-yoshi@intmed2.med.kyushu-u.ac.jp

Received 21 January 2005; revised and accepted 11 April 2005.

INTRODUCTION

Most dura-associated CJD (dCJD) cases have similar clinicopathological features to sporadic CJD (sCJD), presenting progressive mental deterioration, ataxia, myoclonus and characteristic EEG findings such as periodic discharges.¹ However, some patients with atypical dCJD exhibit clinicopathological features distinct from those of most dCJD cases have some resemblance to vCJD cases; that is, a slow progressive clinical course with the absence or late occurrence of periodic discharges on EEG, and the presence of widespread florid plaques in addition to widespread spongiform change, neuronal loss and astrocytosis.^{2–8} On the other hand, the radiological features are different between atypical dCJD and vCJD cases. While vCJD cases present pulvinar high signals compared to all other basal ganglia,^{9,10} atypical dCJD cases have not been reported to show such hyperintensity in pulvinar nuclei.^{2–8} Moreover, the pathological features of the pulvinar nuclei are also different between atypical dCJD and vCJD cases. Here, we report an atypical dCJD case presenting asymmetrical pulvinar hyperintensity on MRI with different pathological characteristics of the pulvinar nucleus from those of reported atypical dCJD and vCJD cases.

CLINICAL SUMMARY

In November 1985, a 9-year-old Japanese girl received a cadaveric dural graft (Lyodura, B Braun Melsungen AG, Germany) at left frontotemporal region following a head injury with brain contusion. Six months later, she had a seizure and anti-epileptic drugs were administered. However, she did not take anti-epileptic drugs regularly, and epilepsy

frequently occurred. From 1995, she gradually developed a violent character. She was diagnosed as suffering a post-traumatic psychosis and received treatment in a psychiatric hospital. In June 2002, 200 months after the procedure, she began to develop an ataxic gait and became bed-ridden. By January 2003, she gradually showed memory disturbance and lost her spontaneous speech and was unable to communicate. She also exhibited myoclonic jerks in her upper limbs. She frequently suffered from aspiration pneumonia, and was brought to our hospital for respiratory insufficiency on 9 April 2003. On admission, she was akinetic and mute with decorticate posturing. There was no apparent history of depression, anxiety, apathy or delusions. Neurological examination showed moderate rigidity in bilateral upper and lower extremities, and myoclonus in bilateral upper extremities. The light reflex, corneal reflex and oculocephalic reflex were all normal. The motor and sensory systems could not be examined in detail. Deep tendon reflexes were normal. There was slow activity without any periodic discharge in her EEG. One week before her death, T2-weighted and proton density-weighted brain MRI showed significant hyperintensity in the thalamic pulvinar nuclei, which was predominantly on the left side, and moderate hyperintensity of the basal ganglia (Fig. 1A,B). Diffusion-weighted and gadolinium(III)-diethyltriaminepentaacetic acid (Gd-DTPA)-enhanced MRI revealed hyperintense signals in the pulvinar (Fig. 1C,D). The brain MRI also presented hyperintense signal by T2-weighted and proton density-weighted images and hypointense signal by diffusion-weighted and Gd-DTPA-enhanced images at the left frontal lobe, corresponding to where the brain contusion existed. In addition, Gd-DTPA enhanced images revealed hyperintense signals at the margin of the brain contusion. Based on the findings of the brain MRI, the diagnosis of dCJD was suspected. However, her respiratory insufficiency progressively worsened and she developed septic shock. Therefore, we could not assess further examination including the cerebrospinal fluid level of the 14-3-3 protein. She died on 19 April, 2003, 10 months after the onset of ataxic gait. The patient's family gave informed consent for the genetic and postmortem studies.

PATHOLOGICAL FINDINGS, IMMUNOBLOTTING AND GENE ANALYSIS

On examination, her brain weighed 1120 g, and there was a large defect in the left basal forebrain. While cerebral atrophy was not obvious, there was substantial atrophy of the cerebellum. The right side of the half-brain was deep-frozen for biochemical examination, and the other half was fixed in buffered formalin. Microscopically, most cerebral

cortices had mild to moderate spongiform changes, neuronal loss, and astrocytosis with a predilection for the deep cortical layers. In contrast, the cingulate gyrus and insular cortex exhibited moderate to severe pathological changes throughout the whole layers. The putamen showed moderate spongiform change, neuronal loss and astrocytosis. Anterior nucleus of the thalamus presented mild spongiform change and neuronal loss, and moderate astrocytosis. Ventral lateral nucleus and dorsomedial nucleus of the thalamus displayed mild spongiform change, moderate neuronal loss and astrocytosis. Pulvinar nucleus of the thalamus exhibited the most severe neuronal loss and spongiform change, and greater astrocytosis than the cerebral cortices (Table 1). The hippocampus was almost completely spared. In the cerebellum, moderate atrophy of the molecular layer was associated with mild spongiform change and astrocytosis, while moderate neuronal loss of the granule layer and severe neuronal loss of the dentate nucleus was associated with moderate astrocytosis. The Purkinje cells were almost completely preserved. In HE sections, we frequently noted Kuru plaques in a number of regions of the cerebral cortex, the putamen and the pulvinar nucleus of the thalamus. The cores of the plaques were stained with PAS, and, when stained with Congo red, appeared apple green in polarized light. In addition, many of the Kuru plaques were surrounded by a zone of vacuolar change, consistent with florid plaques, which are known hallmarks of vCJD. Although the pulvinar nucleus of the thalamus presented frequent Kuru plaques, there were only a few plaques in anterior, ventral lateral and dorsomedial nuclei of the thalamus. Immunohistochemistry for PrP revealed widespread synaptic staining and numerous plaque-like deposits, including florid plaques in all areas of the cerebral cortices, putamen, pulvinar nucleus of the thalamus and white matter of the cerebellum. The globus pallidus, the anterior, ventral lateral and dorsomedial nuclei of the thalamus, and molecular layer of the cerebellum mainly showed synaptic staining associated with mild granular prion protein depositions. In addition, there were PrP deposits surrounding blood vessels, neuronal cell bodies and processes in the cerebral cortex and in the pulvinar nucleus (Fig. 2). The region around the head injury with brain contusion showed mild spongiform change with severe astrocytosis. Only a few Kuru plaques were found in this region (Table 1).

The sequence analysis of prion protein gene (*PRNP*) derived from the brain tissue showed no mutation with homozygous for methionine at codon 129 or for glutamate at codon 219, which are polymorphic sites of the *PrP* gene. Immunoblotting for the abnormal prion protein in the brain demonstrated a type 1 prion protein glycoform pattern (Parchi's classification)¹¹ (Fig. 3). The final diagnosis was atypical dCJD.

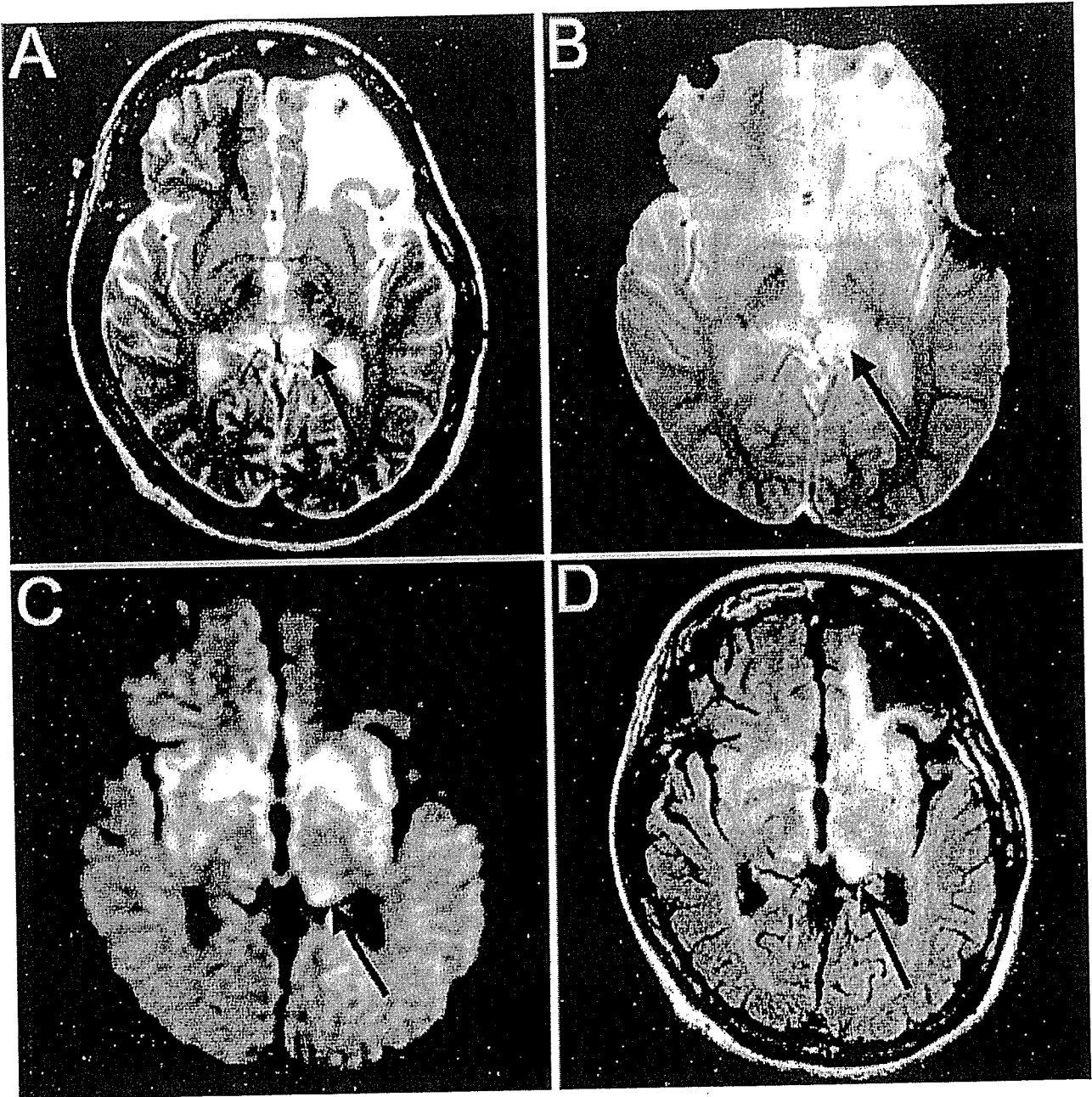


Fig. 1 Neuroradiological images. (A) T2-weighted image, (B) proton density-weighted image, (C) diffusion-weighted image, and (D) gadolinium(III)-diethyltriaminepentaacetic acid (Gd-DTPA)-enhanced brain MRI obtained 1 week prior to death. The images reveal hyperintensity in the pulvinar of the thalamus, and is more apparent in the left side (arrows). Images also show intense bilateral signals in the caudate nuclei and putamen.

DISCUSSION

We present the first atypical dCJD case to show a high pulvinar signal compared with all other basal ganglia on MRI, prominent lesions with severe spongiform changes,

neuronal loss and numerous florid plaques in the posterior thalamus at autopsy.

Most dCJD cases take the form of typical sCJD.¹ Most dCJD cases are clinically evident as a progressive mental deterioration, ataxia and myoclonus. Periodic discharges

are often noted in the EEG before the terminal stage of the clinical course. The disease often progresses rapidly and the clinical course lasts less than 2 years. MRI of dCJD cases has previously shown either normal or non-specific and diffuse brain atrophy.¹² T2-weighted MRI has also shown sCJD cases frequently exhibit symmetrical and hyperintense changes in the putamen and caudate head compared with the thalamus and cerebral cortex.^{13,14} In cases of sCJD, high-intensity signals in the cerebral and cerebellar cortex are also occasionally seen in fluid-attenuated inversion recovery, proton density-weighted and diffusion-weighted MRI-derived images.¹³ Pathologically, the cerebral cortex and cerebellum of dCJD cases are substantially affected. Severe spongiform changes, astrocytosis and neuronal loss are found throughout the brain and cause substantial atrophy, resulting in brain weights of less than 1000 g. Immunohistochemistry reveals diffuse synaptic type deposition of PrP. None or few amyloid plaques are found in the brain.

However, among more than 110 alleged dCJD cases,¹⁵ there have been some atypical dCJD patients with clinicopathological features which are different from those of sCJD and most dCJD cases but share several features with those of vCJD.²⁻⁸ These atypical dCJD and vCJD cases show a slowly progressive clinical course reaching the state of akinetic mutism. The reported duration of atypical dCJD were ranged 5-24 months.²⁻⁸ This duration resembled cases of vCJD, whose duration ranged 8-38 months.¹⁶

In addition, periodic discharges on EEG were commonly absent in both atypical dCJD and vCJD cases. On the other hand, there are several different clinical features between these cases. While most atypical dCJD cases present initially with ataxia and mental deterioration, such as disorientation or memory disturbance often following the ataxia,²⁻⁸ many vCJD cases initially suffer from sensory symptoms including persistent limb pain and/or persistent psychiatric symptoms as depression, anxiety, apathy and withdrawal.¹⁶ Ataxia was reported to develop about 6 months after the onset of psychiatric and sensory symptoms.¹⁶ Moreover, although myoclonus is absent or occurred at the end stage of the disease in atypical dCJD cases, involuntary movements including myoclonus are commonly noted during the clinical course of vCJD cases.¹⁶ The duration of the disease of our case and the absence of periodic discharges on EEG were similar to those features of atypical dCJD and vCJD cases. On the other hand, because our case presented progressive cognitive impairment after the onset of ataxia, and because myoclonus was absent until the end stage of the disease, the clinical course of our case more resembled those of atypical dCJD than vCJD cases.

Pathologically, most atypical dCJD and vCJD cases show widespread spongiform change, neuronal loss and astrocytosis. These pathological changes are mild in the cerebral cortex and severe in caudate nucleus, putamen and cerebellum in both atypical dCJD and vCJD cases.²⁻⁸

Table 1 Neuropathological findings of left side of the half brain

	Spongiform change	Neuronal loss	Astrocytosis	Kuru plaques
MFG	+++	+	++	+++
MTG	+	+	++	++
IPG	+	+	++	+
PVC	+	+	+	++
Cingulate gyrus	+++	++	++	++
Insular cortex	++	++	++	+++
Hippocampus	-	-	-	-
Globus pallidus	+	+	+	-
Putamen	++	++	++	++
Thalamus AN	+	+	++	+
DMN	+	++	++	+
VLN	+	++	++	+
PN	+++	+++	+++	+++
Contusion area	+		+++	+
Cerebellum ML	+		+	-
PCL		-		
GL		++	++	
WM			++	+
DN		+++	++	-

MFG, middle frontal gyrus; MTG, middle temporal gyrus; IPG, Inferior parietal gyrus; PVC, primary visual cortex of occipital lobe; AN, anterior nucleus; DMN, dorsomedial nucleus; VLN, ventral lateral nucleus; PN, pulvinar nucleus; ML, molecular layer; PCL, purkinje cell layer; GL, granular layer; WM, white matter; DN, dentate nucleus.

Spongiform change and neuronal loss are absent (-), mild (+), moderate (++), severe (+++) on HE sections. Astrocytosis and Kuru plaques are absent (-), mild (+), moderate (++), severe (+++) on sections of immunohistochemistry probed with an anti-GFAP antibody (polyclonal, DAKO, Glostrup, Denmark) and antiprion protein antibody (monoclonal, clone 3F4, Senetek, Maryland Heights, MO, USA), respectively.

